The Global Atmosphere and Ocean System, 1994, Vol. 2, pp. 1–20
Reprints available directly from the publisher
Photocopying permitted by license only

SIMULATED VERSUS OBSERVED SEA SURFACE TEMPERATURE IN THE TROPICAL ATLANTIC OCEAN

JACQUES SERVAIN[1,†], ALAIN MORLIERE[2] and CLAUDIO S. PEREIRA[3]
[1]*LODYC-CNRS, Centre ORSTOM, IFREMER, BP 70 29280 Plouzané, France;*
[2]*LODYC-ORSTOM, Université P. & M. Curie, 4 Place Jussieu, 75252 Paris Cedex 05, France;* [3]*CPTEC-INPE, CP 515, São José dos Campos, 12201 SP, Brazil*

The aim of this work was to test the accuracy of simulated sea surface temperature (SST) in the tropical Atlantic Ocean for the period 1982 to 1990 using a three-dimensional primitive-equation oceanic general circulation model. The SST reference was provided by monthly analysis of observed data obtained from selected ships. The annual mean difference between simulated and observed SST did not exceed 1.5 °C, but monthly mean differences of several degrees were found for some areas. There were two main problem areas, one along the western equatorial zone and the other within the northern part of the Gulf of Guinea. The first, characterized by excessively cold SST, corresponded to a westward early shifting of seasonal equatorial surface cooling; and the second, characterized by excessively warm SST, concerned a region of the Gulf of Guinea where winds were light and the sea surface warm. A series of test experiments was performed during one year (1989) using direct measurements of the meteorological variables which enter into the computation of turbulent heat flux forcing, with all other conditions remaining unchanged. The generally disappointing results may relate to the heat flux sensitivity induced by weak variations among basic meteorological variables.

KEY WORDS: Sea surface temperature, tropical Atlantic ocean, simulation, interannual variability

1. INTRODUCTION

Three-dimensional primitive-equation models, such as those of the Geophysical Fluid Dynamics Laboratory (GFDL) (Philander and Pacanowski, 1986; Philander et al., 1987; Leetmaa, 1987) or the Laboratoire d'Oceanographie Dynamique et de Climatologie (LODYC) (Merle and Morlière, 1988; Reverdin et al., 1991) provide satisfactory descriptions of space structures (Siedler et al., 1992) and the seasonal cycle of surface currents (Morlière and Duchêne, 1990) but have certain problems, for example an excessive range in the western basin (Richardson and Philander, 1987). In addition to simulating the seasonal signal, the models can be run to simulate inter-annual oceanic variations (Leetmaa, 1987; Morlière et al., 1989b). Thus, by comparing a multi-year simulation with a complete observed data set, obtained during the 1982–84 FOCAL/SEQUAL experiment, Reverdin et al. (1991) concluded that the considerable deepening of the thermocline characteristic of the 1984 warm event in the Gulf of Guinea was clearly indicated by the LODYC model.

However, descriptive accuracy is not the same for all simulated variables. Even if one perfect oceanic model was available, sea surface temperature (SST) should not be easy to simulate, since it depends mainly on heat flux forcing at the air–sea interface, which is

[†]Present affiliation: ORSTUM/UBO, Centre ORSTOM, B.P. 70, 29280 Plouzané, France

poorly known. Furthermore, uncertainties in the wind forcing can also contribute significantly to SST uncertainties.

Because their direct measurements have been, until now, unattainable over the open ocean, the heat flux terms used to force oceanic primitive-equation models are most often based on climatological factors. This is the case for radiative fluxes and, in particular, latent and sensible heat terms, which are computed by bulk aerodynamic formulae using climatological averages for basic meteorological variables at the air–sea interface. In these formulae, SST is very often provided by the model (as in the LODYC system). Although the estimation of turbulent heat fluxes is not really dependent on sampling frequency (Esbensen and Reynolds, 1981; Hanawa and Toba, 1987), induced SST sensitivity could rise by 0.2 °C (Harrison, 1991) or 0.4 °C (Gent, 1989) due to an inaccuracy of one $W m^{-2}$ in the net heat flux. This is particularly the case in regions with high SST and weak wind (Harrison, 1991). Such sensitivity is reduced tenfold in upwelling regions and where vertical mixing is an important factor.

The wind stress fields used to force oceanic models are usually determined from surface wind observations measured aboard selected ships or from atmospheric model analysis. In the first case, the estimated stress can be significantly different (up to 30%) according to the method used in the time–space averaging process (Hanawa and Toba, 1987). Due to the relative paucity of available surface wind observations, particularly in some areas outside main shipping routes, it is generally impossible to compute stress fields from measurements based on a time-scale of less than a month. This is not really crucial for momentum forcing, because its variability is relatively weak in the tropics and the monthly stress contains most of the signal we wish to study (Servain et al., 1985). The fact that such processing eliminates the high frequency variability of wind forcing is undoubtedly more prejudicial to the calculation of turbulent heat fluxes. One consequence is an underestimation of evaporation in light wind areas. To compensate for this, Philander and Pacanowski (1986) introduced a minimum threshold for evaporation corresponding to the effect of a wind speed of $4.8 m s^{-1}$. In the LODYC model, a similar value ($3.85 m s^{-1}$) corresponds to a minimum threshold of $0.25 dyn cm^{-2}$ for the stress. On the other hand, Leetmaa and Ji (1989) have shown that simulated sea surface and subsurface temperatures, in some regions, may be controlled by the value of the wind drag coefficient. In this respect, Braconnot and Frankignoul (1993), using a multivariable model testing procedure, have shown that the largest source of model uncertainty is drag coefficient indeterminacy.

Here, we wanted to determine if a multi-year experiment using the LODYC model (OPA4 version) could provide a satisfactory simulated SST signal in the tropical Atlantic Ocean. For that purpose, annual, seasonal and interannual SST signals from the simulation were compared with observed SST fields deduced from a ship-of-opportunity database (Servain and Lukas, 1990, hereafter SL). Results from a special experiment using computed input turbulent heat fluxes derived from 1989 ship observations are also discussed. This study was performed as part of the OPERA (Observatoire PERmanent de l'Atlantique tropical) programme which is testing the feasibility of running a real-time model of the tropical Atlantic Ocean in compliance with a TOGA (Tropical Ocean and Global Atmosphere) programme recommendation.

2. GENERAL EXPERIMENTAL CONDITIONS

Driving Forces

The driving forces applied to the system were a wind stress field and total heat flux at the air–sea interface. The wind stress field was based on a monthly analysis of ship observations (SL) from 30° N to 20° S and 60° W to the African coast. Each individual stress vector was computed from each individual observed wind vector before entering into the averaging process. The components τ_x and τ_y of wind stress are given by

$$\tau_x = aC_{dn}S(V_{10})P_x$$

$$\tau_y = aC_{dn}S(V_{10})P_y$$

where
a = air density = $1.2\,\mathrm{kg\,m^{-3}}$
C_{dn} = the drag coefficient for neutral vertical air stratification
$S(V_{10})$ = a corrective term depending on air stability and wind speed at 10 m (V_{10})
P_x, P_y = zonal and meridional components of the pseudo-wind stress ($\mathrm{m^2\,s^{-2}}$) from SL
C_{dn} was derived from Large and Pond (1981):
$C_{dn} = 1.2 \times 10^{-3}\,(0.49 + 0.0065\,V_{10})$ for $11 < V_{10} < 25\,\mathrm{m\,s^{-1}}$
$C_{dn} = 1.2 \times 10^{-3}$ for $V_{10} < 11\,\mathrm{m\,s^{-1}}$.

$S(V_{10})$ was provided by Cardone and Tourre (1987) from a study performed during the FOCAL/SEQUAL experiment in the tropical Atlantic Ocean. Using climatic data from Hsiung (1986), they estimated constant values for the air–sea temperature difference (−1 °C) and relative humidity (80%). Stability dependence resulted in a strong stress increase in light wind conditions ($S > 1.5$ for $V_{10} < 3\,\mathrm{m\,s^{-1}}$), but the effect was rapidly reduced when wind speed increased ($S = 1.09$ for $7 < V_{10} < 8\,\mathrm{m\,s^{-1}}$) becoming negligible for wind speeds above $10\,\mathrm{m\,s^{-1}}$ (Morlière et al., 1989a). The climatological wind stress results of Hellerman and Rosenstein (1983) were used outside the domain of SL observations. A linear interpolation between the two stress fields was performed within an 8°-wide band surrounding the SL observation domain.

The total heat flux input at the air–sea interface is given by the equation

$$F_n = F_{sw} - F_{lw} - F_l - F_s \tag{1}$$

where F_{sw} and F_{lw} are the net downward short-wave and outgoing long-wave radiation budgets respectively, and F_l and F_s are the turbulent surface heat fluxes, namely the latent and sensible heat fluxes.

F_{sw} is essentially a function of cloud cover and daily averaged sun elevation. F_{lw} is influenced by atmospheric water vapour content and cloud cover. F_l is controlled by wind speed, air humidity and both sea and air temperature at the interface, whereas F_s is only controlled by wind speed and the difference between air and sea temperatures.

In the tropical Atlantic Ocean, F_{sw} values are about 150 to $250\,\mathrm{W\,m^{-2}}$ (e.g. Hastenrath and Lamb, 1977; Esbensen and Kushnir, 1981; Oberhuber, 1988). Near the equator, a narrow region of reduced solar heat flux reflects the intertropical convergence zone (ITCZ) and in the subtropics higher values result from lesser cloudiness. Since F_{lw} values contribute a heat loss of typically $-50\,\mathrm{W\,m^{-2}}$, the net radiative budget is a gain for the ocean of about 100 to $200\,\mathrm{W\,m^{-2}}$. With high temperature and

humidity over the tropics, there is considerable oceanic heat loss due to F_l, with maxima (about -100 to $-175\,W\,m^{-2}$) in the areas of strong trade winds. Conversely, F_s is generally low (about $-10\,W\,m^{-2}$) since sea surface and air temperatures do not differ significantly in these regions.

Therefore, total downward heat flux is mainly the residual of solar radiation and latent heat flux. Typical annual mean values for total heat input are $75\,W\,m^{-2}$ in the Atlantic equatorial band (Oberhuber, 1988). Along the west coast of Africa, regions associated with upwelling processes present an annual heat gain. Outside the upwelling regions, i.e., in the open subtropical basins, total downward heat flux changes seasonally from positive values (about $+50\,W\,m^{-2}$) during summer to negative values (about $-50\,W\,m^{-2}$) during winter in both hemispheres.

The Model

The LODYC ocean general circulation model, developed by P. Delécluse and colleagues (Chartier, 1985; Morlière et al., 1989a,b; Madec et al., 1990, 1991; Reverdin et al., 1991) solves the primitive equations under the Boussinesq approximation, assuming hydrostatic equilibrium and a rigid lid. In the OPA4 version of the model, vertical turbulent diffusion is empirically adjusted as in Pacanowski and Philander (1981). Such a parameterization uses a Richardson-number-dependent formulation for both eddy viscosity and eddy diffusivity. To compensate for a deficiency in the high frequency of the monthly winds used, we considered the vertical diffusion coefficient to be equal to its maximum value ($10^{-2}\,m^2\,s^1$) between the first two upper layers of the model, i.e., for the first 20 m of depth. The equatorial thermocline representation was then improved, although probably not enough (see our later discussion). This version of the code extends from one coast of the Atlantic to the other, between 50 °N and 30 °S, which are considered as closed boundaries; more details on the model version are given in Reverdin et al., 1991.

Radiative budgets are provided in the model by the monthly climatology of Esbensen and Kushnir (1981, hereafter EK). Latent and sensible heat fluxes are computed via bulk aerodynamic formulae:

$$F_l = a\,C_l\,V_{10}\,L(0.622/P_a)\,[\mathrm{es}(T_w) - 0.80\,\mathrm{es}(T_a)] \tag{2}$$

$$F_s = a\,C_s\,V_{10}\,C_p(T_w - T_a) \tag{3}$$

where (a and V_{10} are as previously defined)
C_l, C_s = heat exchange coefficients = 1.4×10^{-3}
L = latent heat of evaporation = $2.489 \times 10^6\,J\,kg^{-1}$
P_a = sea-level pressure = 1.013×10^5 Pa
$\mathrm{es}(T) = 10^{(9.4051 - 2353/T)} \times 10^2$ = saturation vapour pressure (in Pa) at temperature T (in degrees Kelvin)
T_w = SST (in degrees Kelvin) given by the model in the previous step
T_a = air temperature (in degrees Kelvin) from EK
C_p = air specific heat = $1004.1\,J\,kg^{-1}\,°C^{-1}$.

The value 0.80 in the F_l equation indicates a relative humidity H equal to 80%.

Initially, the ocean was considered to be at rest, with temperature and salinity as given by the Levitus (1982) climatology (monthly for temperature, seasonally for

salinity). The model was first forced during one year with an annual mean stress (calculated over the 1982–84 period) and then during two years with a monthly mean stress. The simulation was then continued using monthly stress from January 1982 to December 1990. Fields of wind forcing were linearly interpolated at the model time-step (one hour), as were fields of heat flux forcing. Temperature, salinity and current fields for each vertical level were retrieved every five days from the beginning of the real experiment. This nine year simulation provided the SST model data considered here.

SST Observation Field

The SST reference used here was deduced from observations routinely obtained in the tropical Atlantic Ocean by selected ships. The processing to obtain SST monthly fields on a regular grid (2° longitude × 2° latitude) with no gaps is described in SL. Such analysis is similar to that giving the monthly pseudo-wind stress fields used to force the LODYC model dynamically. SST files have been available from January 1964 (Picaut et al., 1985; Servain et al., 1987; SL) to the present day, but this study concerns only the period from 1982 to 1990.

3. 1982–90 SIMULATION RESULTS

Simulated SST fields from 20° N to 20° S and from 60° W to 15° E were averaged monthly into 2° × 2° boxes to allow comparison with ship observations on the same grid. The present discussion is based either on a selection of climatological mapped averages (monthly, seasonally, annually) performed over the entire 1982–90 period (a slight linear space smoothing was used before mapping the data) or on monthly time series related to individual 2° × 2° boxes (without time smoothing) for the same period.

Figures 1 and 2 show some of the initial features of SST simulation relating to the warmest and coldest months in the equatorial area, i.e., April and August respectively. Although the simulated thermal patterns are realistic, SST was obviously too warm in April along the northern coast of the Gulf of Guinea, and too cold in August in the area of equatorial upwelling. This is generalized in Figure 3 which shows the algebraic difference Δ (simulations minus observations) between the long-term means averaged over 108 months (1982–90). The model provides colder SST along the equatorial axis, notably near 25° W ($\Delta < -1.0$ °C), and warmer SST practically everywhere else (Δ about $+0.5$–1.0 °C). Although long-term mean discrepancies did not exceed $|1.5|$ °C, monthly mean discrepancies were occasionally rather large (several degrees Celsius). In the intertropical region, the major difficulty in model SST response concerned an area along the equator east of 20° W, just west of the seasonal equatorial upwelling area, and in June ($\Delta < -2.5$ °C), i.e., during the onset of the 'great' cold season. Such shifting in space–time developments indicates an evident failure of SST simulation in the western part of the equatorial band.

Variations over other regions of the tropical basin were less remarkable. Along the northern Gulf of Guinea, positive discrepancies of up to $+1.5$ °C were spatially confined, with the largest difference between observed and simulated SST occurring in

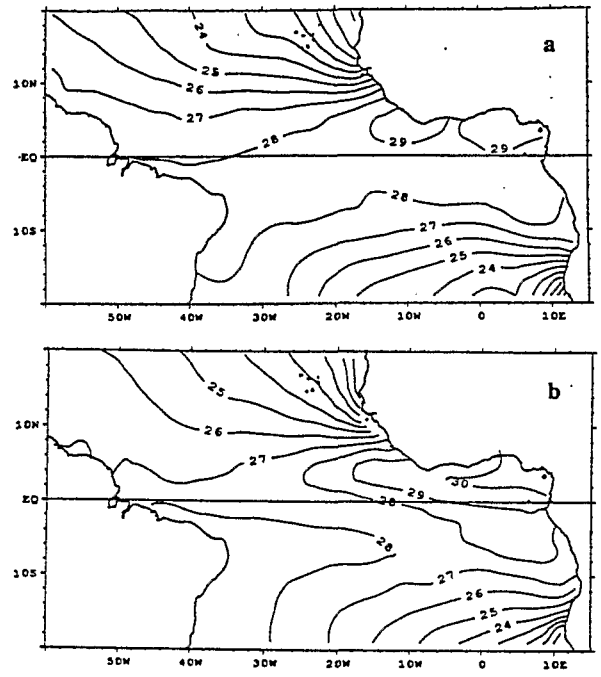

FIGURE 1 a Observed and; b simulated April SST (°C) averaged during the 1982–90 period. The contour interval is 1.

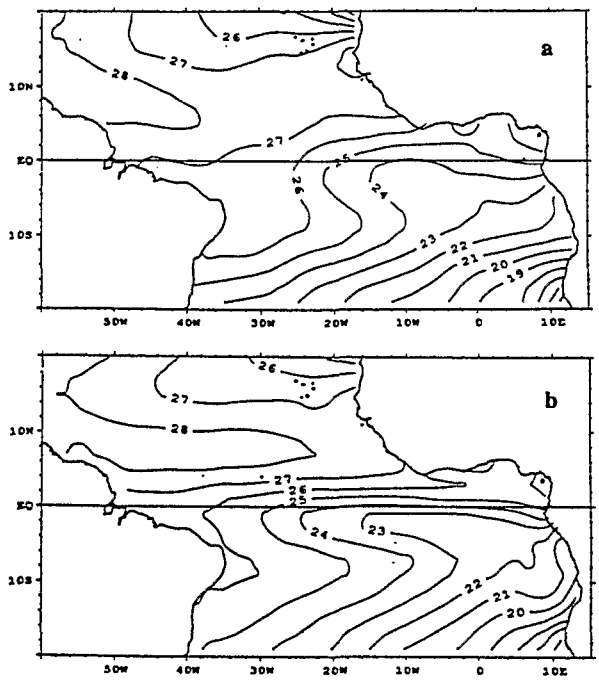

FIGURE 2 a Observed and; b simulated August SST (°C) averaged during the 1982–90 period. The contour interval is 1.

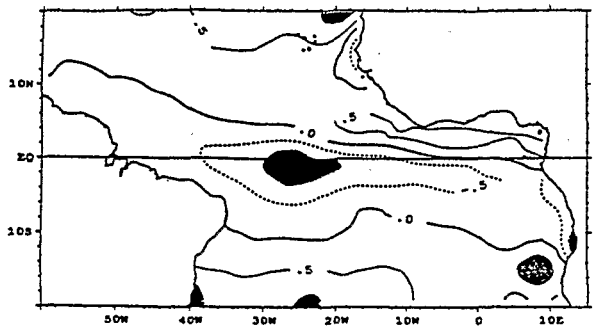

FIGURE 3 Algebraic difference (simulations minus observations in °C) between the long-term means of SST averaged over the 108 months of the 1982–90 period. The contour interval is 0.5, and negative contours are dashed; areas with absolute values greater than 1 are shaded differently according to sign.

February, at the end of the 'small' cold season. Off Senegal (15 °N), the simulated SST climatology was warmer than that observed (about +0.5 °C for monthly averages) from January to April, i.e., during the upwelling season, but colder for the rest of the year, including the warm season (differences exceeding −1.5 °C in June and November). In the Angola upwelling region (10° S), simulated SST remained too cool throughout the year, with a maximum difference (up to −1.0 °C) in September–October. Elsewhere, the discrepancies between the annual means of simulated and observed SST were generally less than |0.5| °C.

The observed SST standard deviation was computed from the 108 months of the 1982–90 period and is given in Figure 4a. Maximum variabilities were noted in the upwelling regions. The root mean square (RMS) of the sea surface temperature, also computed from the 108 months of the 1982–90 period, confirmed the previously noted model deficiencies, e.g., along the equator between 20° W and 30° W (RMS > 1.5 °C) as well as in the vicinity of the coastal upwellings off Senegal and Angola (Figure 4b). The deduced skill factor map (Figure 4c) is the ratio of the RMS to the standard deviation of the observations. It indicates once more the difficulty of providing simulation for the western equatorial Atlantic Ocean (skill factor > 1). Outside this region, the RMS between simulated and analysed SST remained smaller than the variance in observations.

The four time series (1982–90) of the simulated and observed monthly mean SST presented in Figure 5 were selected to lie in the open low-latitude ocean, according to their geographical interest and the aforementioned questionable results. Figure 5a illustrates that the annual range of simulated SST, close to the equator and 27° W, was too large. Moreover, computed values were almost always colder than observed values, and the cold season began too early in the year (though there was no significant time-lag for the onset of the warm season). Such a deficiency was less important in the vicinity of the seasonal equatorial upwelling, close to 10° W (Figure 5b), where the annual range of simulated SST corresponded roughly to that of observed SST. Although simulated SST was again always colder than that of observations, variations were not as great as further west. Practically no time-lag between simulated and observed SST signals was noted during the entire study period. The other time series

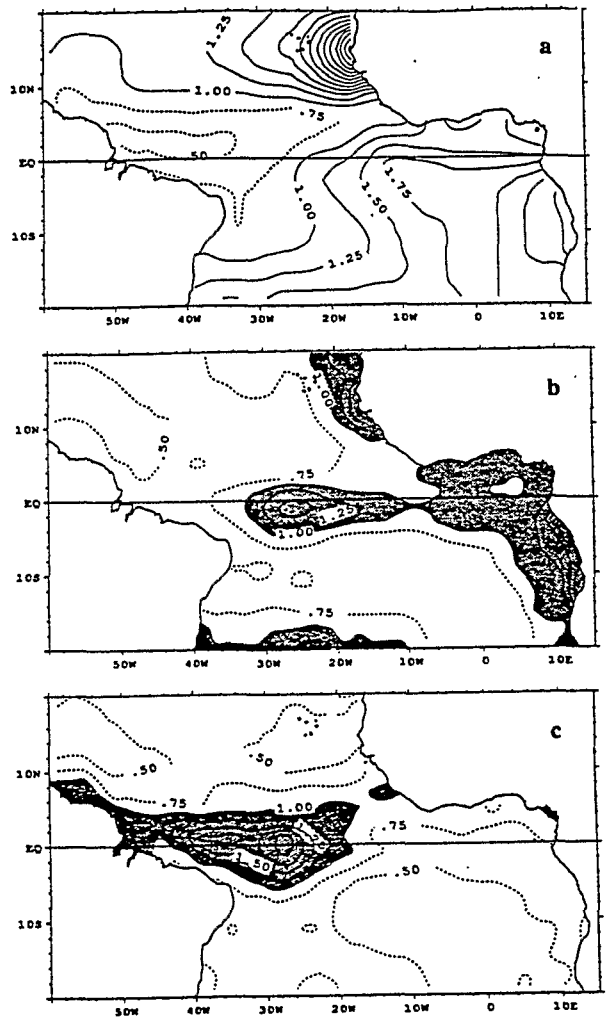

FIGURE 4 a Standard deviations (°C) of observed SST; b RMS (°C) of simulated versus observed SST; and c skill factor. All computations were performed over the 108 months of the 1982–90 period. Contour intervals are 0.5 for (a); 0.25 for (b) and (c); values greater than 1 are shaded for (b) and (c).

(Figures 5c, d) show the 1982–90 SST signals for two boxes selected respectively within the northern and southern equatorial basins. The quality of SST simulation varied, but no systematic errors occurred as in the two previous cases. The amplitude and phase of the simulated seasonal signal were valid. For the northern example (Figure 5c), the main problem was a tendency for the model to overrun (± 1.5 °C) simulated SST values during the warm season of the first-half of the study period. For the southern example in the Gulf of Guinea (Figure 5d), SST was correctly simulated. However, great climatic differences, e.g. the considerable warming in 1984 (Philander, 1986; Servain and Séva, 1987; Hisard, et al., 1986; Shannon, et al., 1986), were poorly simulated. There was thus

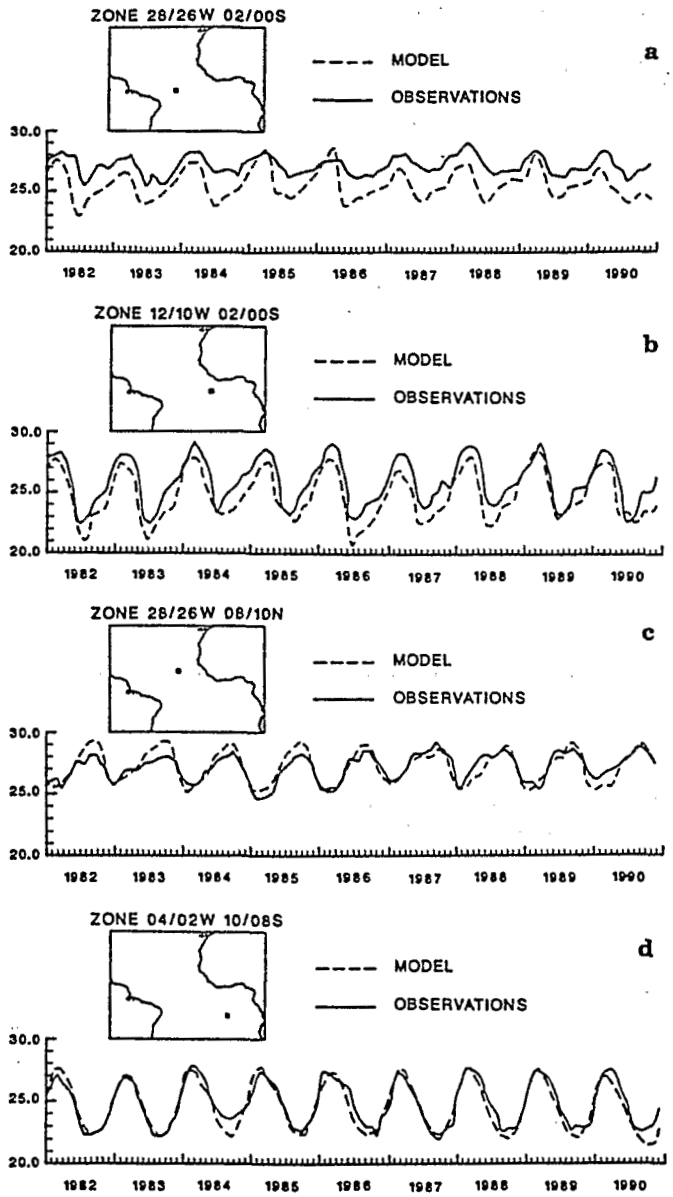

FIGURE 5 **a, b, c and d** Four examples of observed (solid) and simulated (dashed) SST monthly time series (°C) during 1982–90. The 2° × 2° box location is mapped for each example.

a great discrepancy between observed and simulated annual averages for that region in 1984.

Zero-lag correlation coefficients (CC) between anomalous time series for simulated and observed SST were computed for each of the 2° × 2° boxes. Only a few non-extended areas (not shown) had significant CC, and most of these were in the northern

basin. Even though the model accuracy could be considered satisfactory for a multi-month average, in terms of the skill factor (Figure 4c), the model was still largely inadequate for simulation of SST anomalies on a monthly time scale.

4. A SPECIAL EXPERIMENT FOR 1989

Specific Experimental Conditions

Two series of tests can be used in an attempt to improve the SST simulation. They are complementary but can be conducted independently. One series of tests is related to more sophisticated formulations and structures in the model code (other people at LODYC are presently in charge of such developments) while the other series of tests consists of using more realistic forcing patterns; in particular, the wind stress and heat flux inputs. In this paper we limited the study to a test of model sensitivity when turbulent heat flux inputs from climatic values were replaced by turbulent heat flux inputs issued from meteorological values observed aboard ships of opportunity. Note that the cloud cover data reported by ships are very few and are not well suited for radiative calculations. The test was carried out during 1989 only, and this year was chosen because it was at the end of our study period and also because climatic conditions for SST were nearly normal that year. Thus, the 1989 monthly anomaly patterns for observed SST in the tropical Atlantic Ocean (anomaly computed versus 1964–89 SST climatology) changed from a meridional dipole (Servain, 1991) with a cold northern and warm southern structure until May 1989, to an inverse situation at the end of the year. From July to September 1989, the SST was warmer than normal throughout most of the basin. However, SST differences computed during 1989 rarely exceeded a monthly mean of 1.5 °C. As shown in Figure 6a, the 1989 SST abnormality was not comparable, for instance, with the warm episodes which occurred during 1988 and, in particular, during 1984 (SL, Servain et al., 1987).

Three simulations were performed during 1989 using three different turbulent heat fluxes; all other conditions, notably wind forcing and radiative heat flux, remained unchanged:

(i) a control run (CR) forced by the turbulent heat flux, computed as described in the preceding section

(ii) an intermediate run (IR) forced by the turbulent heat flux, computed from observed values for T_a and H instead of a climatological value for T_a and a constant value for H (80%)

(iii) a run, referred to as RR, forced by the turbulent heat flux computed from observed values for all basic meteorological variables.

The SST used with the bulk formulae was provided by the model for CR and IR, and directly by observations for RR.

The five basic meteorological variables used in the computation of net heat flux came from observations: T_w (or SST), T_a, V_{10}, P_a and H. H was computed from the depression of the dew-point, i.e. the difference between air temperature (T_a) and the dew-point. For each variable, the twelve monthly fields of the year 1989 were arranged

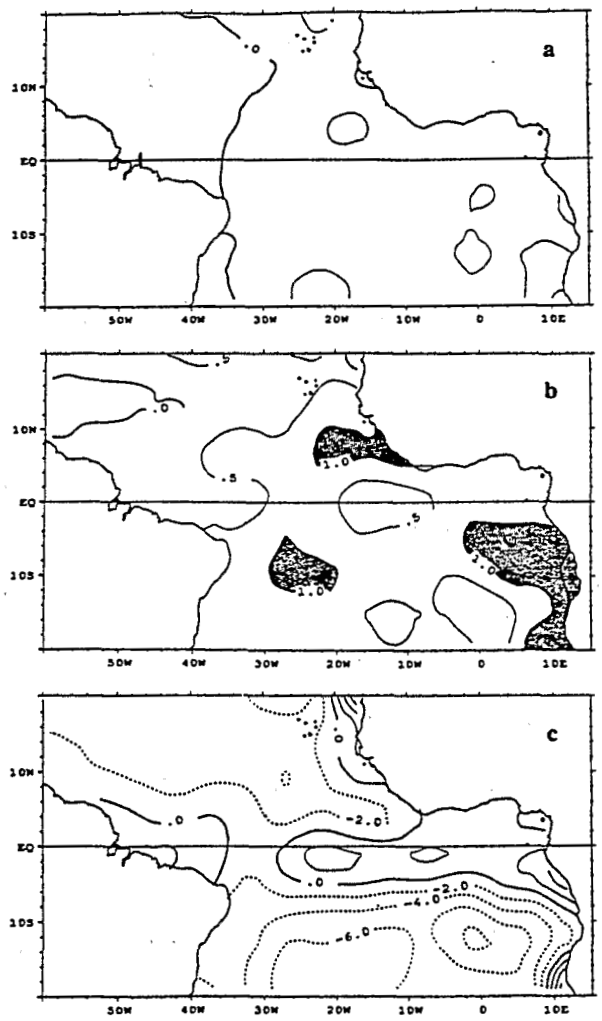

FIGURE 6 a Annual deviations (°C) for 1989 observed SST versus climatic SST given by SL; b annual deviations (°C) for observed T_a versus climatic T_a given by EK; and c annual deviations (%) for observed H versus 80%. Contour intervals are 0.5 for (a) and (b) and 2 for (c); negative contours are dashed, while areas with absolute values greater than 1 are shaded for (a) and (b).

over a 2° latitude by 2° longitude grid, with no gaps. SST fields were previously available (SL), and the fields for other variables were determined using processing similar to that for SST (for further details, see Servain et al., 1987). This method included objective analysis according to the Cressman (1959) scheme and required monthly climatologies for each variable. Except for SST, the climatologies used were derived from the COADS (Woodruff *et al.*, 1987) in accordance with a remodelling process by Oberhuber (1988). The main difficulty in setting the mean monthly fields arose from the nonuniform density of available observations for the variables (Table 1). For instance, the amount of data for the depression of the dew-point represented only

TABLE 1

Available observed data during 1989 for each variable.

Month	SST	T_a	P_a	V_{10}	H
January	7464	7305	7375	7471	3966
February	6572	7294	7145	7215	3795
March	7030	7783	7829	7624	4277
April	6445	7395	7321	7230	4286
May	6671	8157	8146	7087	4700
June	5474	6414	6368	6207	3704
July	6410	7229	7177	6971	4111
August	6424	7422	7352	7186	4422
September	6336	7120	7095	6847	4651
October	6452	7179	7256	7042	4135
November	6770	6896	6994	6768	3939
December	6768	7458	8386	7225	4050
Mean	6568	7304	7370	7073	4170

55 to 60% of that of the air temperature data. One result of this was that the difference in the accuracy of the basic variable fields was not easy to estimate. Another consequence was the obligation to use the first averaged meteorological observations in the calculations of heat flux patterns instead of averaging individual heat fluxes as calculated from individual basic observations. Although these problems can arise in inherent non-linear turbulent bulk formulae, Esbensen and Reynolds (1981) have shown that such circumstances are not really prejudicial to monthly time-scale computations for turbulent heat fluxes (this is not the case for stress).

The 1989 monthly fields of latent and sensitive heat fluxes were performed within the same $2° \times 2°$ grid used for basic meteorological variables. Bulk aerodynamic equations similar to Eqs. (2) and (3) were used, but with some improvements in RR computations. Thus, the exchange coefficients for latent and sensible heat Fluxes were not considered as constant but as varying with wind speed and atmospheric stability above the sea surface (Liu et al., 1979). Furthermore, air density varied with air temperature, atmospheric pressure at sea level and specific humidity.

From CR to IR Experiments

Figures 6b and 6c summarize the differences in input conditions between CR and IR experiments. As for SST (Figure 6a) the measured air temperature was generally about 0.5 to 1.5 °C warmer in 1989 (Figure 6b)—especially for the eastern basin—than in the climatology according to EK. Annual mean relative humidity for 1989 was 80% ±2%, except for south of 10° S (values below 74%) and near a few coastal areas (Figure 6c).

Similar to our previously noted findings for the entire 1982–90 period, SST in the 1989 control run proved colder than observed SST (about 0.5 to 1.0 °C) along the equatorial axis, especially between 20° W and 30° W, and along the African coast between 18° N and 8° N. Elsewhere, CR-simulated SST was around 0.5 °C warmer than observed SST. A small difference was noted (Figure 7a compared with Figure 7b)

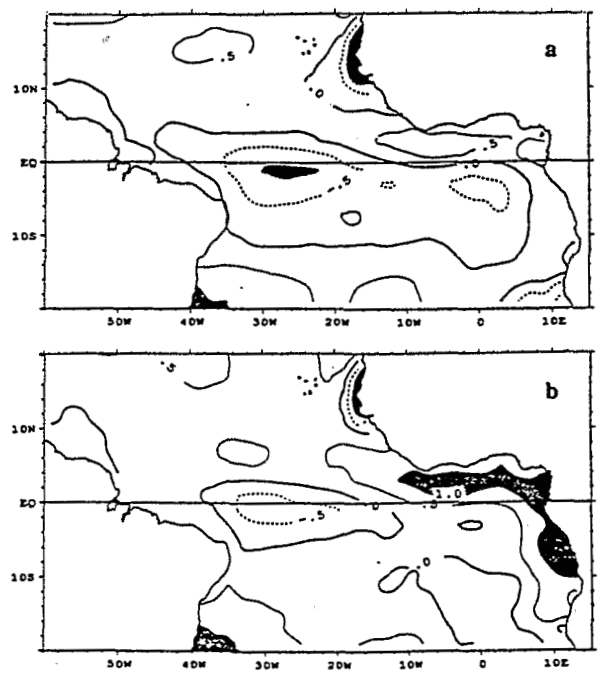

FIGURE 7 **a** 1989 annual deviations (°C) for CR-simulated versus observed SST, and **b** 1989 annual deviations (°C) for IR-simulated versus observed SST. The contour interval is 0.5, and negative contours are dashed, while areas with absolute values greater than 1 are shaded differently according to sign.

between the simulated SST of CR and IR experiments for open ocean regions at latitudes extending to 10° N and 10° S. Inside the equatorial band and along the African coast, the differences were more substantial: the IR SST field was warmer than the CR SST field, so that differences with observations were less than 1 °C for IR in the western equatorial region but greater than 1 °C along the northern and eastern Gulf of Guinea.

From CR to RR Experiments

The subsequent discussion is related to net turbulent heat flux exchange ($F_n = F_s + F_l$). As sensible heat values remain weak compared with latent heat (below 10%) this discussion will, obviously, mainly concern the latter.

Along the equatorial axis, net turbulent oceanic heat flux loss in the CR experiment (Figure 8a) was about 10% lower than in the RR experiment (Figure 8b). Outside the equatorial zone the situation was reversed: negative heat flux values in CR were generally about 10 to 20% greater than those in RR. As a result, the meridional gradient of the heat flux exchanges from the equator towards higher latitudes was greater for the control run. From CR through RR (Figure 8c), oceanic heat loss increased up to 20 W m^{-2} along the equatorial axis (particularly from 15° W to 35° W, with a maximum during the period June to August) and in the vicinity of the Dakar

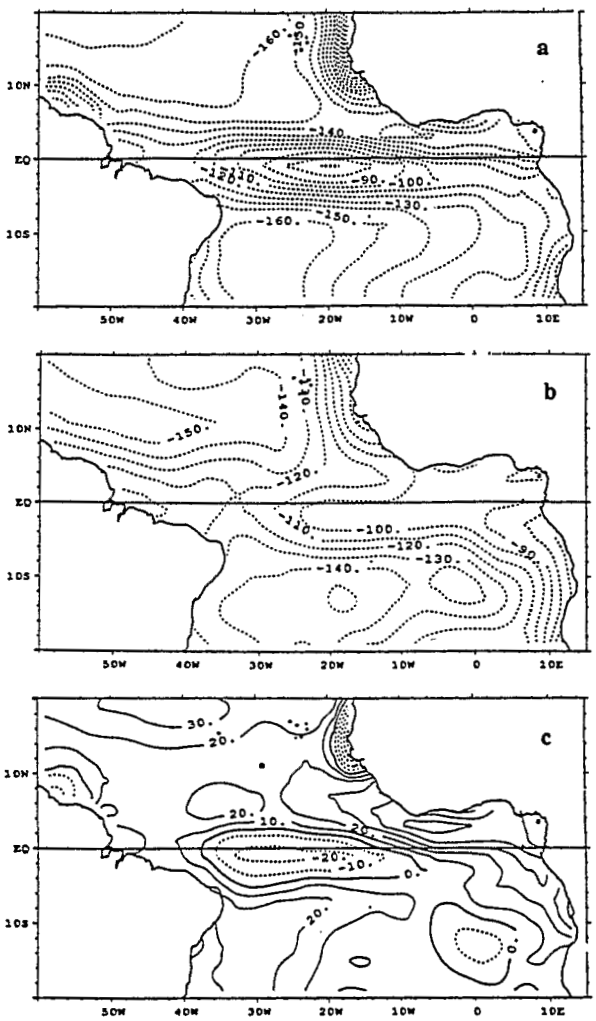

FIGURE 8 1989 annual mean net heat flux computed by a CR; b RR; and c RR minus CR. The contour interval is 10 W m^{-2}, and negative contours are dashed.

upwelling. However, the loss was limited elsewhere, especially in the heart of the Gulf of Guinea where differences could exceed 50 W m^{-2}, with a maximum during the period January to March. Such circumstances (higher loss in the western equatorial zone, lower loss in the Gulf of Guinea) unfortunately reduced the validity of the RR experiment by comparison with the previous results. Figure 9 is similar to Figure 7b, but with the replacement of IR by RR. It demonstrates that SST simulation by the RR experiment was totally unrealistic. In fact, the main defects of SST simulation were amplified, leading mainly to additional warming (several degrees Celsius) in the Gulf of Guinea where positive deviations were previously recorded. The questionable results of this special 1989 experiment are considered in the following section.

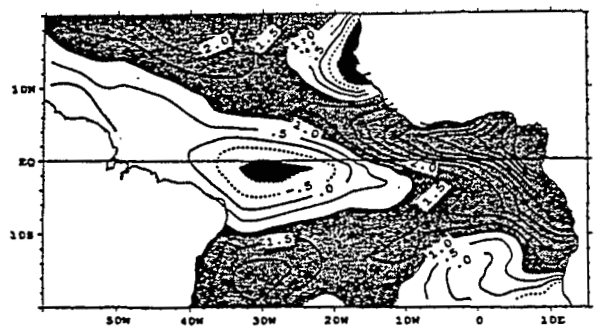

FIGURE 9 1989 annual deviations (°C) for RR-simulated versus observed SST. Contour intervals are 0.5 and negative contours are dashed, while areas with absolute values greater than 1 are shaded differently according to sign.

5. DISCUSSION AND CONCLUSION

Our main objective was to test the capacity of the LODYC 3D oceanic model to simulate the interannual signal of SST in the tropical Atlantic Ocean. The model was first forced during a multi-year period (1982–90) by monthly wind stress fields derived from observations, and by radiative and turbulent heat flux fields derived from climatic basic variables. In a test experiment during one year (1989) the previous turbulent heat flux forcing was replaced by realistic turbulent heat flux deduced from basic meteorological observations.

The results were both promising and disappointing. They were encouraging because, for large oceanic domains, the RMS difference integrated throughout the entire 1982–90 period, between simulated and observed SST, was lower than the natural variability of observations. However, there were notable failures, most of which resulted in systematic and/or seasonal errors and concerned the domain studied. The western equatorial band indicated the major problem (Figure 4c). Does this local failure mostly appear related to variation in turbulent heat flux input? From the present results, it seems the answer is negative. A calculation performed from the data fields of Figures 7a, 8c and 9 allowed us to estimate quickly that a change of 1 $W m^{-2}$ (see Figure 8c, at about 28 W–30 W) produced a variation in of SST sensitivity of less than 0.02 °C (consider the departure between Figures 7a and 9, at about 28 W–30 W). This value is considerably weaker than those values calculated by Gent (1989) and Harrison (1991). However, to answer the question with certainty, it would be necessary to reintegrate the model with various 'artificial' values of heat flux, assuming an equal change of at least 10 $W m^{-2}$ all over the basin.

We think the primary cause responsible for reducing the accuracy of the simulated SST signal along the western equatorial zone arose from a direct modelling problem, expressed by a westward early shifting in the seasonal cooling equatorial core. Indeed, spatial and temporal deviations were confirmed (data not shown in this paper) by an analysis of the simulated subsurface thermal signal. Furthermore, for the natural SST variability, being minimal in this western equatorial zone (see Figure 4a), whichever model is used would have difficulty in providing precise simulations of such slight variations.

The heart of the Gulf of Guinea was also a region where SST simulation with the LODYC model proved questionable. At the climatic average, the skill factor may be considered reasonable since it showed that the RMS difference between the model data and the observations was lower than the variance in observations (Figure 4c). However, the model efficiency was strongly devalued at the interannual scale (Figure 5). This region is particularly sensitive to heat flux input modifications, with a variation of $1\,W\,m^{-2}$ leading to estimated errors of more than 0.1 °C in monthly SST (i.e. five times higher than in the western equatorial band). A mixing layer thickness with the current version of the LODYC model, that was not fully adequate, could have increased limitations in the simulated mixing processes for such heat flux sensitive regions. Another previously discussed reason is the poor assessment of the dynamic effect due to the weak values of the wind field developing in this region. In addition, the lack of a high frequency signal in the monthly analyzed wind forcing was necessarily detrimental to the modelling experiments.

We tested the sensitivity of the net turbulent heat flux (F_n) to the variations of some units around each 1989 monthly observed situations of V_{10}, T_a, SST and H, respectively. All the results were then regressed to variations of ± 1 unit in order to obtain an estimation of the slope of sensitivity around the observed average of each basic variable. Annual slope coefficients ($W\,m^{-2}$) of net turbulent heat flux, when one basic parameter uniformly varies by a single positive unit ($m\,s^{-1}$ for wind velocity, °C for T_a and SST) from its observed value and all the other variables remain unchanged, are presented in Figure 10. For a uniformly negative variation of one unit, the patterns should be similar (for weak variations the heat transfer processes are practically linear) but with opposite signs. The sensitivity of turbulent heat flux was relatively constant ($\pm 17\,W\,m^{-2}$) over the entire study area for a wind velocity change of $\pm 1\,m\,s^{-1}$ (Figure 10a) or a T_a change of ± 1 °C (Figure 10b). Compared with that, the sensitivity of the turbulent heat flux for a SST change of ± 1 °C was three times as great (Figure 10c). The SST change effect remains one and a half times greater than the wind change effect if we consider, as suggested by Sarachik (1984), that typical ship errors are 1 °C in SST (and T_a) and $2\,m\,s^{-1}$ in V_{10}. Furthermore, a greater spatial dependence was noted in the case of the SST change effect, with maxima ($>55\,W\,m^{-2}$) in the regions of strong trade wind velocity and minima ($<45\,W\,m^{-2}$) along the African coast. Note that the effect of humidity change was weak: a variation of $\pm 1\%$ of H led to mean variations (not shown) in net turbulent heat flux of $\pm 5\,W\,m^{-2}$. These results are in agreement with those of Weare (1989) who showed from weather report data that uncertainties in latent heat flux over the tropical Pacific Ocean could exceed $30\,W\,m^{-2}$.

In our special experiment for 1989, the radiative flux remained climatic and we did not look at its uncertainty. The cloud cover data provided by selected ships is too sparse to produce gridded patterns. This does not mean we assumed the radiative flux was correct. However, because the shortwave flux is as large, or larger than the latent flux component of the heat budget, its uncertainty is not negligible. Recently, Busalacchi (1992) showed that the 1984 warm event in the Gulf of Guinea could have been induced both by a dynamic relaxation of remote wind stress and a local solar flux anomaly.

In conclusion, the LODYC 3D oceanic model, forced by observed wind stress and climatic heat flux, was not able, at least in the current OPA4 version, to simulate

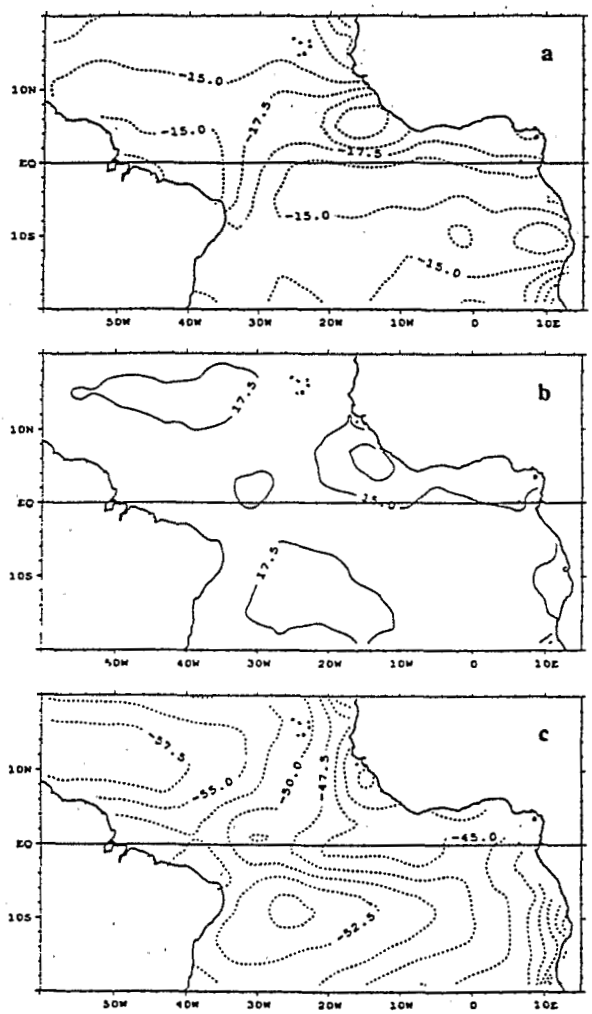

FIGURE 10 1989 annual slope coefficients ($W m^{-2}$) for net turbulent heat flux variation induced by a one-unit positive change around the observed values of **a** V_{10}; **b** T_a and **c** SST (the sign of coefficients must be reversed for a one-unit negative change).

correctly an interannual signal of the SST over the tropical Atlantic. The failure was even more pronounced when we tested this model as being forced by turbulent heat flux derived from direct basic measurements instead of heat fluxes calculated with model and climatic data. It was apparent that relatively slight variations in these variables can cause significant changes in heat flux values computed according to bulk formulae. Among these basic observed variables, SST is a parameter of major importance since indeterminacies in the magnitude of V_{10} or T_a are not as crucial. All these uncertain values entering into the oceanic model can cause substantial errors in the simulated heat content of the surface layer and, in simulated SST.

Accordingly, a considerable effort is required to increase the number of basic observations (including the cloud cover) and to minimize their errors. This must happen in the immediate future with the operational use of satellite observations and their assimilation within the traditional observation system. For instance, studies are now underway to improve the quality and sampling of the wind data provided by the satellite ERS1. Another means of improving simulation would involve sophistication of the model code, particularly to provide a better mixing process for the oceanic subsurface layer. A new version of the LODYC model now being tested uses a vertical mixing scheme proposed by Gaspar et al. (1990). The initial results (Blanke and Delécluse, 1993) show significant progress in simulating SST response along the equator and within the Gulf of Guinea. This new version of the model code is now employed in the OPERA programme.

Acknowledgments

Computer resources on Cray 2 were provided by the 'Centre de Calcul Vectoriel pour la Recherche'. Funds for data analysis were provided by ORSTOM, CNRS and IFREMER (Project OPERA No. 91.1.430.023) under the supervision of the 'Programme National pour l'Etude de la Dynamique du Climat'. Claudio Pereira's six month work period at the ORSTOM Center in Brest was facilitated by an ORSTOM grant.

References

Blanke, B. and Delécluse, P. (1993). Variability of the Tropical Atlantic Ocean simulated by a general circulation model with two different mixed-layer physics. *Journal of Physical Oceanography*, **23**, 1363–1388.

Braconnot, P. and Frankignoul, C. (1993). Testing model simulations of the thermocline depth variability in the tropical Atlantic from 1982 through 1984. *Journal of Physical Oceanography*, **23**, 626–647.

Busalacchi, A.J. (1992). Personal communication.

Cardone, V. and Tourne, Y. (1987). Personal communication.

Chartier, M. (1985). Un modèle numérique tridimensionnel aux équations primitives de circulation générale de l'océan. *Thèse de doctorat d'université*, Université P. et M. Curie, Paris, France.

Cressman, G.P. (1959). An operational objective analysis system. *Monthly Weather Review*, **87**, 367–374.

Esbensen, S.K. and Kushnir, Y. (1981). The heat budget of the global ocean: an atlas based on estimates from marine surface observations. *Climatic Research Institution*, Report No. 29, Oregon State University, Corvallis, OR, USA.

Esbensen, S.K. and Reynolds, R.W. (1981). Estimation monthly averaged air–sea transfers of heat and momentum using the bulk aerodynamic method. *Journal of Physical Oceanography*, **11**, 457–465.

Gaspar, P., Grégoris, Y. and Lefevre, J.M. (1990). A simple eddy-kinetic-energy model for simulations of the ocean vertical mixing: tests at station Papa and long-term upper ocean study site. *Journal of Geophysical Research*, **95**, 16179–16193.

Gent, P. (1989). A new ocean GCM for the tropical ocean and ENSO studies. *Proceeding of the Western Pacific International Meeting on TOGA COARE*. (Eds. J. Picaut, R. Lukas and T. Delcroix), ORSTOM BPA5, Noumea, New Caledonia, pp. 445–463.

Hanawa, K. and Toba, Y. (1987). Critical examination of estimation methods of long-term mean air-sea heat and momentum transfers. *Ocean-Air Interactions*, **1**, 79–93.

Harrison, D.E. (1991). Equatorial sea surface temperature sensivity to net surface heat flux: some ocean circulation model results. *Journal of Climate*, **4**, 538–549.

Hastenrath, S. and Lamb, P.J. (1977). *Heat Budget Atlas of the Tropical Atlantic and Eastern Pacific Oceans*. University of Wisconsin Press, Madison, WI, USA.

Hellerman, S. and Rosenstein, M. (1983). Normal monthly windstress over the world ocean with error estimates. *Journal of Physical Oceanography*, **13**, 1093–1104.

Hisard, P., Henin, C., Houghton, R., Piton, B. and Rual, P. (1986). Conditions in the tropical Atlantic Ocean during 1983 and 1984. *Nature*, **322**, 243–245.

Hsiung, J. (1986). Mean surface energy flux over the global ocean. *Journal of Geophysical Research*, **91**, 10585–10606.

Large, W.G. and Pond, S. (1981). Open ocean momentum flux measurements in moderate to strong winds, *Journal of Physical Oceanography*, **11**, 324–336.

Leetmaa, A. (1987). Progress toward an operational ocean model of the tropical Pacific at NMC/CAC. In *Further Progress in Equatorial Oceanography* (Eds. E.J. Katz and J.M. Witte), Nova University Press, FL, USA, pp. 439–450.

Leetmaa, A. and Ji, M. (1989). Operational hindcasting of the tropical Pacific. *Dynamic Atmospheres and Oceans*, **13**, 465–490.

Levitus, S. (1982). *Climatological Atlas of the World Ocean*, NOAA prof. Paper 13, US Government Printing Office, Washington DC.

Liu, W.T., Katsaros, K.B. and Businger, J.A. (1979). Bulk parameterization of air–sea exchanges of heat and water vapor including the molecular constraints at the interface. *Journal of Atmospheric Science.*, **36**, 1722–1735.

Madec, G., Chartier, M. and Crepon, M. (1990). The effect of thermohaline forcing variability on deep water formation in the western Mediterranean sea: a high-resolution three-dimensional numerical study. *Dynamics Atmospheres and Oceans*, **15** (3–5), 301–332.

Madec, G., Chartier, M., Delécluse, P. and Crepon, M. (1991). A three-dimensional numerical study of deep water formation in the northwestern Mediterranean sea. *Journal of Physical Oceanography*, **21**, 1349–1371.

Merle, J. and Morlière, A. (1988). Toward an operational 3-dimensional simulation of the tropical Atlantic Ocean. *Geography Research Letters*, **15**, 653–656.

Morlière, A. and Duchêne, C. (1990). Evaluation des courants de surface d'un modèle de circulation générale de l'Atlantique tropical. *Rap. Interne LODYC*, 90/11, p. 32.

Morlière, A., Delécluse, P., Andrich, P. and Camusat, B. (1989a). Une évaluation des champs thermiques simulés par un modèle de circulation générale dans l'atlantique tropical. *Oceanologica Acta*, **12**, 9–22.

Morlière A., Reverdin, G. and Merle, J. (1989b). Assimilation of temperature profiles in a general circulation model of the tropical Atlantic. *Journal of Physical Oceanography*, **14**, 1892–1899.

Oberhuber, J.M. (1988). An atlas based on the 'COADS': the budgets of heat, buoyancy and turbulent kinetic energy at the surface of the global ocean. *Report 15, Max-Planck Institute für Meteorologie*, Hamburg, Germany.

Pacanowski, R.C. and Philander, S.G.H. (1981). Parameterization of vertical mixing in numerical models of tropical oceans. *Journal of Physical Oceanography*, **11**, 1443–1451.

Philander, S.G.H. (1986). Unusual conditions in the tropical Atlantic Ocean in 1984. *Nature*, **322**, 236–238.

Philander, S.G.H. and Pacanowski, R.C. (1986). A model of the seasonal cycle in the tropical Atlantic ocean. *Journal of Geophysical Research*, **91**, 14192–14206.

Philander, S.G.H., Hurlin, W. and Siegel, A.D. (1987). A model of the seasonal cycle in the tropical Pacific Ocean. *Journal of Physical Oceanography*, **17**, 1986–2002.

Picaut, J., Servain, J., Lecomte, P., Séva, M., Lukas, S. and Rougier, G. (1985). *Climatic Atlas of the Tropical Atlantic Wind Stress and Sea Surface Temperature* 1964–1979. Université de Bretagne Occidentale—University of Hawaii, Brest, France.

Reverdin, G., Delécluse, P., Levy, C., Morlière, A. and Verstraete, J.M. (1991). The near surface tropical Atlantic in 1982–1984. Results from a numerical simulation and a data analysis. *Progress in Oceanography*, **27**, 273–340.

Richardson, P. and Philander, S.G.H. (1987). The seasonal variations of surface currents in the tropical Atlantic Ocean: a comparison of ship drift data with results from a general circulation model. *Journal of Geophysical Research*, **92**, 715–724.

Sarachik, E.S. (1984). Large scale surface heat fluxes. In *Large-scale Oceanographic Experiments and Satellites* (Eds. C. Gautier and M. Fieux), D. Reidel Publishing Co., pp. 147–165.

Servain, J. (1991). Simple climatic indices for the tropical Atlantic Ocean and some applications. *Journal of Geophysical Research*, **96**, 15137–15146.

Servain, J. and Legler, D.M. (1986). Empirical orthogonal function analyses of tropical Atlantic sea surface temperature and wind stress: 1964–1979. *Journal of Geophysical Research*, **91**, 14181–14191.

Servain, J. and Lukas, S. (1990). *Climatic Atlas of the Tropical Atlantic Wind Stress and Sea Surface Temperature* 1985–1989. SDP IFREMER edition.

Servain, J. and Séva, M. (1987). On relationships between tropical Atlantic sea surface temperature, wind stress and regional precipitation indices: 1964–1984. *Ocean–Air Interactions* 1, 183–190.

Servain, J., Picaut, J. and Busalacchi, A.J. (1985). Interannual and seasonal variability of the tropical Atlantic ocean depicted by sixteen years of sea surface temperature and wind stress. In: *Coupled Ocean Atmosphere Models* (Eds. J.C.J. Nihoul), Amsterdam, Elsevier pp. 211–237.

Servain, J., Séva, M., Lukas, S. and Rougier, G. (1987). Climatic atlas of the tropical Atlantic wind stress and sea surface temperature: 1980–1984, *Ocean–Air Interactions* **1**, 109–182.

Shannon, L.V., Boyd, A.J., Brundit G.B. and Tauton-Clark, J. (1986). On the existence of an El Niño type phenomenon in the Benguela system. *Journal of Marine Research*, **44**, 495–520.

Siedler, G., Zangenberg, N., Onken, R. and Morlière, A. (1992). Seasonal changes in the tropical Atlantic circulation: observation and simulation of the Guinea dome. *Journal of Geophysical Research*, **97**, 703–715.

Weare, B.C. (1989). Uncertainties in estimates of surface heat fluxes derived from marine reports over the tropical and subtropical oceans. *Tellus*, **41A**, 357–370.

Woodruff, S.D., Slutz, R.J., Jenne, R.L., and Steurer, P.M. (1987). A comprehensive Ocean-Atmosphere data set. *Bull. Amer. Meteor. Soc.*, **68**, 1239–1250.